chemistry

MDPI

Article

Dehydration of Fructose to 5-Hydroxymethylfurfural: Effects of Acidity and Porosity of Different Catalysts in the Conversion, Selectivity, and Yield

João Pedro Vieira Lima [1], Pablo Teles Aragão Campos [1], Mateus Freitas Paiva [1], José J. Linares [2], Sílvia C. L. Dias [1] and José A. Dias [1,*]

[1] Laboratório de Catálise, Instituto de Química, Campus Universitário Darcy Ribeiro, Universidade de Brasília, Asa Norte, Brasília 70910-900, DF, Brazil; jpvieiralima123@gmail.com (J.P.V.L.); pablo.teles1998@gmail.com (P.T.A.C.); freitas-paiva@hotmail.com (M.F.P.); scdias@unb.br (S.C.L.D.)

[2] Laboratório de Desenvolvimento de Processos Químicos, Instituto de Química, Campus Universitário Darcy Ribeiro, Universidade de Brasília, Asa Norte, Brasília 70910-900, DF, Brazil; joselinares@unb.br

* Correspondence: jdias@unb.br or josediasunb@gmail.com; Tel.: +55-61-3107-3846; Fax: +55-61-3107-3900

Abstract: There is a demand for renewable resources, such as biomass, to produce compounds considered as platform molecules. This study deals with dehydration of fructose for the formation of 5-hydroxymethylfurfural (HMF), a feedstock molecule. Different catalysts (aluminosilicates, niobic acid, 12-tungstophosphoric acid—HPW, and supported HPW/Niobia) were studied for this reaction in an aqueous medium. The catalysts were characterized by XRD, FT-IR, N_2 sorption at −196 °C and pyridine adsorption. It was evident that the nature of the sites (Brønsted and Lewis), strength, quantity and accessibility to the acidic sites are critical to the conversion and yield results. A synergic effect of acidity and mesoporous area are key factors affecting the activity and selectivity of the solid acids. Niobic acid ($Nb_2O_5 \cdot nH_2O$) revealed the best efficiency (highest TON, yield, selectivity and conversion). It was determined that the optimum acidity strength of catalysts should be between 80 to 100 kJ mol^{-1}, with about 0.20 to 0.30 mmol g^{-1} of acid sites, density about 1 site nm^{-2} and mesoporous area about 100 m^2 g^{-1}. These values fit well within the general order of the observed selectivity (i.e., Nb_2O_5 > HZSM-5 > 20%HPW/Nb_2O_5 > SiO_2-Al_2O_3 > HY > HBEA).

Keywords: biomass; fructose dehydration; 5-hydroxymethylfurfural (HMF); solid acids; niobia; aluminosilicates

Citation: Lima, J.P.V.; Campos, P.T.A.; Paiva, M.F.; Linares, J.J.; Dias, S.C.L.; Dias, J.A. Dehydration of Fructose to 5-Hydroxymethylfurfural: Effects of Acidity and Porosity of Different Catalysts in the Conversion, Selectivity, and Yield. *Chemistry* **2021**, *3*, 1189–1202. https://doi.org/10.3390/chemistry3040087

Academic Editors: Tomas Ramirez Reina and Gianguido Ramis

Received: 14 September 2021
Accepted: 8 October 2021
Published: 12 October 2021

1. Introduction

Human society's current energy dependence on fossil and non-renewable sources (predominantly oil and natural gas) is indisputable and is growing [1–4]. In this scenario, several environmental and social complications have arisen, such as air pollution and global warming [2,5]. An alternative that has gained prominence in recent decades is biomass, which is basically any and all natural organic matter that can be used to produce energy. It is constantly generated in nature, starting with the fixation of the carbon present in the air in carbohydrates, through the process carried out by plants and known as photosynthesis [6]. The advantages of using biomass as an alternative energy source to fossil sources are diverse (e.g., abundance resources, natural replacement), in addition to lower pollution during burning of fuels [7,8].

The chemical composition of biomass includes carbohydrates, compounds that can be used directly for conversion to fuels. In this process, an intermediary deserves to be highlighted: 5-hydroxymethylfurfural (HMF), which is considered a platform molecule [9–11]. This means that it acts as an intermediary for several products of extreme value for industry and society, for instance 2,5-dimethylfuran acid (DMF) and levulinic acid [9], both with great energy potential, and 2,5-furanedicarboxylic acid (FDCA), a precursor of the polymer polyethylene furanoate (PEF), a substitute for PET plastics [11].

The primary method of obtaining HMF is from the biomass dehydration reaction, being in general produced from glucose and fructose monomers. Dehydration of sugars involves homogeneous and heterogeneous catalysts, such as sulfuric acid, zeolites, polyoxometalates, ionic liquids, etc. [10,12,13]. Because of the easier separation, lower corrosion of the reactor and recyclability of the catalyst, heterogeneous catalysis has achieved industrial notoriety [14]. Besides obtaining fructose from biomass, it is worth noting that various types of waste (e.g., beverage) have considerable amounts of this molecule. Therefore, they could be used as a starting point for the reaction, building a sustainable practice of valorization of industrial and social waste. Fructose production processes from food and beverage waste have already been described in the literature [15], in which the authors report the production of low-cost fructose syrup using beverage waste. The overall fructose recovery efficiency was about 78%. Then, the recovered fructose could be further transformed into HMF.

The reaction mechanism of HMF formation from fructose involves triple dehydration. On the other hand, when the starting point is glucose, it must first undergo isomerization to fructose, and then follow the same route as before [16–18]. Numerous undesirable side reactions can and will occur, mainly in aqueous media, generating mostly organic acids and humins (oligomers resulting from polymerization reactions between molecules of reactants, products and intermediates) [11,16].

A challenge in fructose dehydration is the reaction medium, because of the low values of selectivity and yield. Thus, the literature has several studies with many solvents, especially dimethyl sulfoxide (DMSO) and methyl isobutyl ketone (MIBK) [10,11,14,19,20], although those are not considered green [21]. One of the reasons that may justify the low yield in an aqueous medium is the ease of rehydration of the HMF to levulinic and formic acids [9,22], in addition to the water allowing several parallel and consecutive reactions, which are suppressed when using DMSO, for example. However, the use of water brings several advantages, such as representing a green protocol for obtaining HMF, reduction in solvent costs and greater ease of separation [23].

The acidic properties of different catalysts have been pointed as a crucial effect on the yield for fructose dehydration [9,24,25]. However, much less emphasis has been placed on the effect of the textural properties on the accessibility of active sites. For instance, a recent paper about sulfonic acid on titania-based catalysts (TiO_2-SO_3H) investigated the dehydration of fructose to HMF, showing very high conversion and selectivity at 1.1 mol L^{-1} fructose concentration at 165 °C, which were attributed to a counterbalance between the acidity and pore structure of the catalytic sites [26].

Thus, the present work aims to present the results of fructose dehydration in an aqueous medium for HMF using different catalysts, correlating catalytic activity with acidic and textural properties. Synergic effects of acidity and porosity, which affect shape selectivity, are examined as key factors of the different solid acids. Fructose is considered a model molecule of biomass, which has been studied in its transformation to important platform molecules under different solvents.

2. Materials and Methods

2.1. Preparation of the Catalysts

The following catalysts were used in the dehydration reactions: zeolites Y, *BEA and ZSM-5; amorphous silica-alumina (SiO_2-Al_2O_3); hydrated niobium pentoxide (niobic acid, $Nb_2O_5 \cdot nH_2O$) and 12-tungstophosphoric acid hydrate ($H_3PW_{12}O_{40} \cdot nH_2O$, HPW). The zeolites—Y (CBV 300, SiO_2/Al_2O_3 mole ratio = 5.1), BEA (CP814E, SiO_2/Al_2O_3 mole ratio = 25) and ZSM-5 (CBV 2314, SiO_2/Al_2O_3 mole ratio = 23), obtained from Zeolyst International in ammonium form, were calcined at 550 °C (8 h) to convert them into the protonic form. Amorphous silica-alumina in ammonium form (Sigma-Aldrich, Burlington, MA, USA, SiO_2/Al_2O_3 mole ratio = 12.4) was also subjected to the same thermal treatment. $H_3PW_{12}O_{40} \cdot nH_2O$, HPW) was purchased from Sigma-Aldrich, 99.9%, USA, and used without any purification or thermal treatment. The niobic acid ($Nb_2O_5 \cdot nH_2O$, CBMM—

Companhia Brasileira de Mineração e Metalurgia, Araxá, Brazil) was thermally heated at 100 °C (1 h). The 20% HPW/Nb_2O_5 sample was prepared by impregnation in aqueous acid solution (HCl 0.1 mol L^{-1}). The obtained solid was calcined at 300 °C for 4 h. All calcinations were performed in a micro-processed muffle furnace (model Seven, EDG, Passa Quatro, Brazil) under static air conditions in porcelain crucibles. Each catalyst was pressed, crushed and sieved to ≤200-mesh fraction for the characterization and reaction tests.

2.2. Characterization of the Catalysts

Powder diffraction patterns were obtained in a powder diffractometer (model D8 Focus, θ–2θ, Bruker, Karlsruhe, Germany) using CuKα = 0.15418 nm radiation. The acquisition included operating at 40 kV and 30 mA, scanning rate of 1° min^{-1} at 0.05° increments.

FT-IR spectra were collected using a spectrometer (model 6700, Nicolet, Thermo Fisher Scientific, Waltham, MA, USA). The conditions were: 256 scans and a resolution of 4 cm^{-1} under transmittance mode (KBr pellets).

The nature of acid sites was obtained by FT-IR measurements of chemisorbed pyridine on the catalysts. Pellets with 10 wt.% of catalyst, previously adsorbed with pyridine, were prepared in a N_2 glove box, placed in a holder and taken straight to the FT-IR spectrometer (recorded at 25 °C). Immediately before the measurements, gas-phase pyridine was adsorbed on the catalyst using a custom-made glass fixed bed reactor in situ experiment. The catalysts (~20 mg) were first dried at 300 °C for 2 h under vacuum in the reactor and then cooled to 100 °C. Gaseous pyridine diluted in dry N_2 was subsequently flowed over the samples for 1 h. The reactor was then heated and maintained at 150 °C for 1 h to remove all physically adsorbed pyridine.

The textural data (specific surface area, pore-volume and area distribution) were acquired through gaseous N_2 physisorption isotherms at −196 °C using a surface area analyzer equipment (ASAP 2020C, Micromeritics, Norcross, GA, USA). Approximately 0.5 g of the solid catalyst was treated for 8 h at 200 °C under a high vacuum (~10^{-5} mbar) before analysis. The isotherms were fitted to different models to calculate the specific surface area (BET), and the distribution of areas to compute the total area (micropores + external + mesopores) were obtained by t-plot (microporous and external) and BJH (mesoporous). The estimated errors were based on the S_{BET} measurements ($3\sigma S_{BET}$), i.e., approximately ±15 m^2 g^{-1}. All basic structural characterization is provided as supplementary data.

The acidity of the catalysts was obtained by studying the heat evolved from pyridine adsorption in the liquid phase using cyclohexane slurries measured by microcalorimetric titrations. The activated catalysts were suspended in anhydrous cyclohexane and incremental addition of diluted pyridine solution in cyclohexane was added by a syringe pump to the slurry. The heat evolved was measured using a calorimeter (model ISC 4300 from Calorimetry Sciences Corporation-CSC, Linden, UT, USA). The interval between pyridine additions was 4–5 min, which is sufficiently long for equilibrium to be achieved. Additional detailed procedures and calculations have been described elsewhere [27].

2.3. Catalytic Dehydration of Fructose

In a typical experimental reaction, 1.0 g of fructose and 100 mg of catalyst (catalyst/fructose ratio = 10 wt.%) were weighed and placed in a polytetrafluoroethylene (PTFE, Teflon) liner, followed by the addition of 30 mL of deionized water (obtained by purification using Milli-Q system, Merck Millipore, Burlington, MA, USA). The PTFE liner was inserted in a stainless-steel autoclave, where the reaction was maintained at 120 °C for 2 h using an oil bath and under magnetic stirring (600 rpm). After completion, the autoclave was cooled with the aid of running water and an aliquot was withdrawn from the reaction medium for analysis. Before analyzing the aliquot from the reaction, it was centrifuged at 3400 rpm for 30 min to separate the solid catalyst and then filtered out using a 0.22 μm syringe filter.

2.4. Analysis by High-Performance Liquid Chromatography (HPLC)

Fructose (Neon Commercial, 98%, São Paulo, Brazil) and HMF (Sigma-Aldrich, 99.9%, USA) were analyzed in the filtered liquid phase using HPLC. The equipment (LC-20A Prominence Modular HPLC, Shimadzu, Kyoto, Japan) was supplied with a refractive index detector (RID) and diode array detector (DAD), in addition to a Shim-Pack SCR-101H chromatographic column. The mobile phase used was a solution of sulfuric acid (Merck, 98%, Rio de Janeiro, Brazil) with a concentration of 12.5 mmol L^{-1} and a flow of 1.0 mL min^{-1}, for 25 min at a temperature of 80 °C. The remaining fructose after the reaction and the formed HMF were quantified by integration of the area under the corresponding peak obtained by RID and correlating it with an analytical curve made with a standard solution of each substance (Supplementary Materials Figure S1).

Conversion, which is related to the final concentration of fructose, was calculated by Equation (1):

$$C = \frac{[\text{Fructose}]_i - [\text{Fructose}]}{[\text{Fructose}]_i} \times 100\% \quad (1)$$

where $[\text{Fructose}]_i$ and [Fructose] are the initial and final concentrations (mol mL^{-1}) of fructose, respectively.

Yield was defined by Equation (2):

$$Y = \frac{[\text{HMF}]}{[\text{Fructose}]_i} \times 100\% \quad (2)$$

where [HMF] is the concentration (mol mL^{-1}) of HMF at the end of the reaction.

Finally, selectivity was calculated by the ratio Y/C (Equation (3)), i.e.,

$$S = \frac{Y}{C} \times 100\% = \frac{[\text{HMF}]}{[\text{Fructose}]_i - [\text{Fructose}]} \times 100\% \quad (3)$$

3. Results and Discussion

The dehydration of fructose was studied in the presence of different catalysts in an aqueous solution, being initially evaluated in terms of conversion of the starting material, selectivity and yield for the formation of HMF (Table 1). A quantitative method for fructose and HMF determination was developed by HPLC using the analytical curves for each substrate (Supplementary Materials Figure S1). Analytical contour maps obtained by HPLC are shown in Figure 1, demonstrating the typical result found for all catalysts.

Table 1. Conversion (fructose), selectivity and yield (HMF) for the different catalysts in aqueous solution [a].

Catalyst	Conversion (%) [b]	Selectivity (%)	Yield (%)	CB (%) [c]
No catalyst	24.9	3.7	0.9	76.0
HBEA	17.2	6.6	1.1	84.0
HY	12.0	8.8	1.1	89.1
HZSM-5	13.7	17.2	2.4	88.6
SiO_2-Al_2O_3	15.4	11.1	1.7	86.3
Nb_2O_5 (amorphous)	47.5	28.9	13.7	66.2
20%HPW/Nb_2O_5	53.9	13.4	7.2	53.3
HPW	19.3	34.6	6.7	87.4

[a] Reaction conditions: 120 °C, 2 h; 1.0 g fructose; 0.1 g catalyst; 30 mL deionized water. [b] The relative error on the fructose conversion is ±2% based on triplicate experiments. [c] CB = Carbon Balance: proportion of carbon detected after the reaction (residual fructose carbon plus HMF carbon). The difference to 100% carbon is associated with the formation of humins and other by-products.

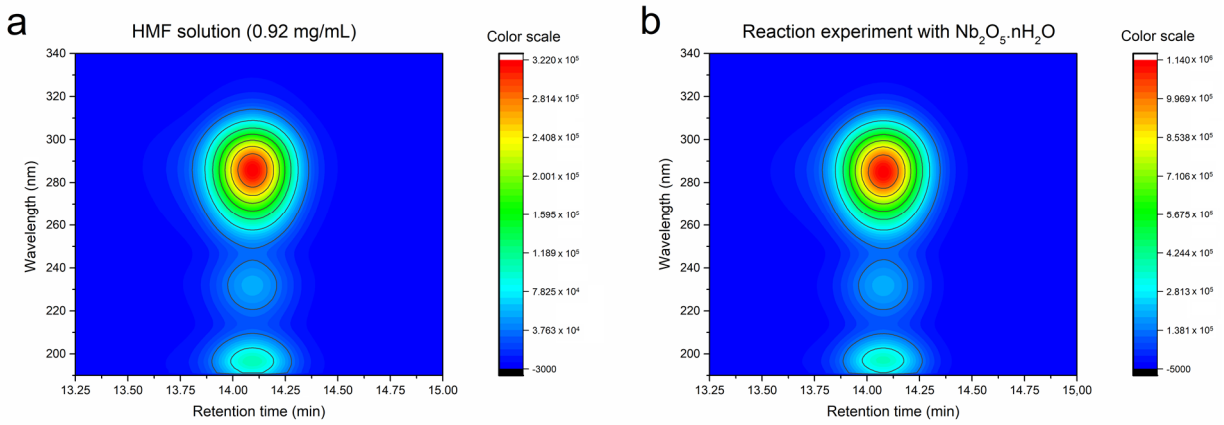

Figure 1. Typical contour map obtained for the HMF produced from the fructose dehydration reaction. (**a**) The left panel represents a standard solution of HMF (0.92 mg mL^{-1}), whereas (**b**) the right panel corresponds to a sample from the reaction with niobic acid.

A quick comparison among the solid acid catalysts under the same experimental conditions shows that amorphous Nb_2O_5 has the highest conversion and yield, whereas using HPW (homogeneous process) renders the highest selectivity to HMF. Among the aluminosilicates, different trend orders can be observed for conversion and selectivity. The conventional conversion of fructose to HMF involves mainly two types of acid sites (Brønsted and Lewis), with Brønsted sites being considered more important in the dehydration of hexoses [11,27–34]. The calculated activation energy of that conversion in aqueous neutral pH is about 310 kJ/mol, which is very high and, in the absence of a catalyst, leads to a slow reaction [11]. According to the classical reactions proposed in the literature (e.g., [9,29]), Scheme 1a–c represents a simplified mechanism of the process and its multiple challenges. In (a), the actual mechanism is difficult to assign because the starting fructose can be in various isomer forms and depending on the solvent it can act as a catalyst for that isomerization [29]. In (b), possible intermediates during the reaction are indicated, which is also very dependent on the solvent [12,30]. In (c), important by-products are shown, such as levulinic and formic acids that are produced by rehydration of HMF [9,31,34]. Accordingly, structural and reactivity parameters are analyzed in the following sections to explain the results as observed in Table 1. Different groups of tested catalysts are considered, to better define their main properties that might influence the reaction and its products.

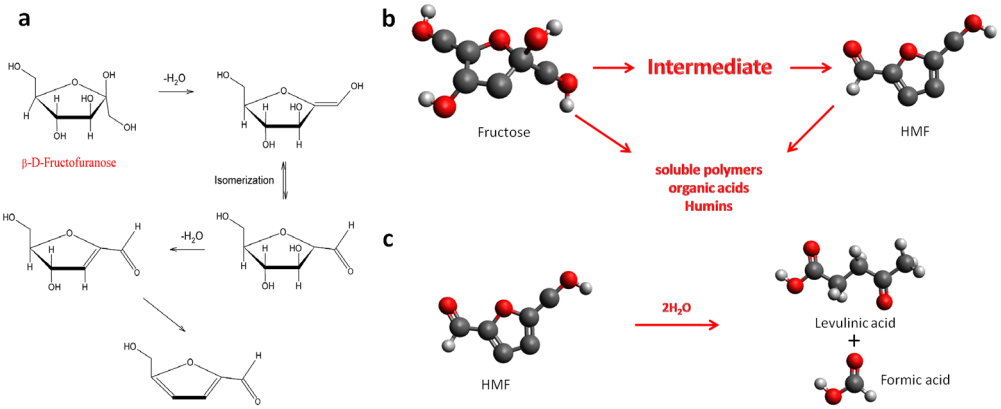

Scheme 1. Some processes related to dehydration of fructose to HMF in acid solution. (**a**) Possible fructose isomerization; (**b**) transformation of fructose to HMF and the presence of intermediates; (**c**) import by-products obtained by rehydration of HMF.

3.1. Crystalline and Amorphous Aluminosilicate Materials

Aluminosilicates are typical solid acids used in a variety of reactions. The acidity, texture, structure and morphology are important properties related to their activity in heterogeneous catalysis [35–39]. The structure of the studied aluminosilicates was confirmed by XRD (Figure S2). The nature and quantity of Brønsted and Lewis acid sites (BAS and LAS) in aluminosilicates can be probed by pyridine and verified by FT-IR (Figure S3). The FT-IR spectra demonstrate the accessibility of pyridine (Py) on both types of sites. The quantity (n_{Py}) and strength (ΔH) of the sites, which were obtained by microcalorimetry, are presented in Table 3. The total quantity of available acid sites (n_{OH}) can be obtained by the thermogravimetric method according to the Zhuravlev model [40], but the accessed sites are usually obtained by an adsorbed basic probe (e.g., pyridine). We observed that the total acid sites (n_T) and the density of acidic sites (α_{Py}) accessed by pyridine follows the order: SiO_2-Al_2O_3 > HZSM-5 > HBEA > HY (e.g., Table 3, n_T = 0.85, 0.58, 0.53, and 0.33 mmol g^{-1}, respectively), but the acidic strength order for the strongest sites is: HZSM-5 > HBEA > HY > SiO_2-Al_2O_3 (i.e., $-\Delta H_1$ = 170, 150, 143, and 81 kJ mol^{-1}, respectively). Clearly, the higher density of sites (i.e., α_{Py} order: SiO_2-Al_2O_3 > HZSM-5 > HBEA > HY) does not mean that they will have greater selectivity (i.e., HZSM-5 > SiO_2-Al_2O_3 > HY > HBEA) and conversion (i.e., HBEA > SiO_2-Al_2O_3 > HZSM-5 > HY) of fructose, since not every site will be able to react, due to steric effects, competition for sites and diffusion of reactants and products during the reaction time. In addition, side reactions might compromise the observed selectivity to HMF. The kinetic size of the Py is usually taken in the literature as 0.54 nm, and thus larger molecules such as cyclic fructose and HMF (kinetic sizes of ~ 0.86 and 0.82 nm, respectively) will have limited access to the main sites or restricted diffusion along the microporous channels, which will facilitate side reactions to take place. It is known that zeolites with different acid site strengths and site densities may produce various types of mechanisms, and consequent activities. Furthermore, there is a synergic effect between acidity and porosity that causes shape selectivity in many hydrocarbon reactions [41] or other reactions in different solvents [42].

A careful analysis of the amount of Py that accesses the strongest sites (n_1, Table 3) identifies that HZSM-5 has the smallest number of accessible ones, but this zeolite has the lowest pore diameter that may prevent the probe from reaching all the sites. A textural profile, based on the adsorption/desorption isotherms (Figure S4) of the catalysts (Table 2) and the total area distributions (Figure 2), may also give insights into this effect. Thus, the strongest acidic sites act to generate the highest dehydration rate and the higher rate of dehydration prevents fructose side reactions, as well as condensation reactions from HMF [43]. It is claimed that a higher density of Brønsted sites increases the number of positive charges in fructose, accelerating the catalytic process and increasing selectivity [44]. However, this amount of Brønsted sites should be of adequate strength, even though only the strength does not explain the observed selectivity or even the conversion order of the aluminosilicates.

Amorphous SiO_2-Al_2O_3 shows the highest amount of mesoporous surface area, as well as the total number of acid sites (n_T). This indicates that these sites are probably the most accessible and that fructose can diffuse within the pores avoiding stereo hindrance and encountering less competition for those sites, which explains the higher conversion, even though selectivity was not very high. However, the transformation is probably slower, because of the lower strength of the acid sites. This hypothesis suggests that parallel transformation of fructose in the mesopores of this catalyst leads to oligomeric by-products, as indicated in the literature [19,45]. This is supported by our results of carbon balance (CB), which shows SiO_2-Al_2O_3 and HBEA (the aluminosilicates with higher mesoporous area) forming the largest quantity of humins and by-products.

Table 2. Textural properties of catalysts obtained from N_2 adsorption/desorption isotherms at −196 °C.

Catalyst	S_{BET} [a] ($m^2\ g^{-1}$)	V_p [b] ($cm^3\ g^{-1}$)	$V_{\mu p}$ [c] ($cm^3\ g^{-1}$)	D_{XRD} [d] (nm)
SiO_2-Al_2O_3	489	0.69	-	n.a.
HY	813	0.34	0.32	69
HBEA	754	0.79	0.23	22
HZSM-5	438	0.26	0.11	118
Nb_2O_5	122	0.13	0.02	n.a.
20%HPW/Nb_2O_5	52	0.06	0.01	n.a.

[a] Specific surface area obtained by the BET method ($0.02 < p/p_0 < 0.2$). The standard error (2σ) was $\pm 5\ m^2\ g^{-1}$. [b] Total pore volume obtained by the amount of gas adsorbed at $p/p_0 = 0.98$. [c] Microporous volume obtained by t-plot method. [d] Crystallite domain size obtained by XRD using Scherrer's equation (±5 nm).

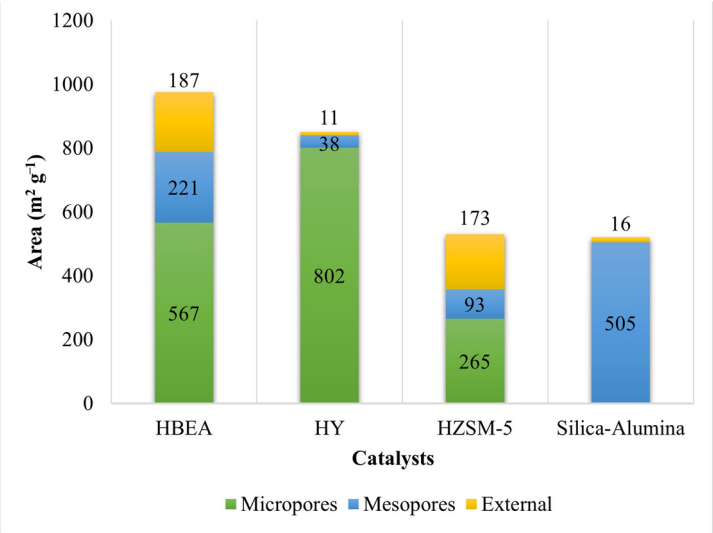

Figure 2. Distribution of specific surface areas of the aluminosilicate catalysts.

Table 3. Strength of the acid sites ($-\Delta H_i$) [a] obtained by microcalorimetry of pyridine adsorption (two-site model reaction) in cyclohexane, the total number of reactive acid sites ($n_T = n_1 + n_2$) [b] and density of adsorbed Py (α_{Py}) [c].

Catalyst	$-\Delta H_1$ (kJ/mol)	$-\Delta H_2$ (kJ/mol)	n_1 (mmol/g)	n_2 (mmol/g)	n_T (mmol/g)	α_{Py} (Py/nm^2)
SiO_2-Al_2O_3	81	44	0.20	0.65	0.85	1.05
HY	143	74	0.11	0.22	0.33	0.24
HBEA	150	63	0.15	0.38	0.53	0.42
HZSM-5	170	36	0.05	0.53	0.58	0.80
Nb_2O_5	88	50	0.06	0.15	0.21	1.00
20%HPW/Nb_2O_5	85	45	0.09	0.19	0.28	2.48

[a] Errors for $-\Delta H_1$ and $-\Delta H_2$ are ± 1 kJ mol^{-1}; Data adapted from references [46–50]. [b] Errors for n_1 and n_2 are ±0.01 and 0.02 mmol g^{-1}, respectively. [c] $\alpha_{Py} = n_{Py} \times NA \times 10^{-18}/S_{BET}$; where: n_{Py} ($10^{-3} \times$ mmol g^{-1}); NA is the Avogadro constant; S_{BET} is the BET specific surface area ($m^2\ g^{-1}$); and 10^{-18} is a conversion from m^2 to nm^2. Errors are ± 0.01 Py nm^{-2}.

The dehydration for HMF in zeolite HBEA is a balance between the number of the strongest sites and the number of EFAL (extra framework aluminum) species, i.e., the

presence of Lewis sites. The relatively higher number of secondary mesoporous in this zeolite reflects better accessibility to the acidic sites. Further, EFAL species analyzed by ^{27}Al MAS NMR (solid state magic angle spinning nuclear magnetic resonance) [26] may help to explain the higher conversion of fructose to HMF on this zeolite. However, the low selectivity is probably due to the rapid secondary reaction of the HMF molecules adsorbed within the pores of this zeolite [44]. In this case, the presence of characteristic Lewis acid sites also catalyzes the reaction of the transformation of HMF into humins, as previously pointed out. Besides this, because of the relatively high mesoporosity of this zeolite, there is a faster diffusion of fructose that accesses the sites. Thus, there might be the formation of fructose dimers that are not transformed into HMF, reducing the selectivity, which is also evidenced by observation of side reactions in other studies [13,51]. Thus, it is reasonable to say that, in the case of HBEA, HMF was being generated, but a substantial part of it was consumed during the experiment because of the high number of strong and accessible acid sites i.e., HBEA has a larger number of stronger sites (n_1), as well as larger pores and mesoporous area than HZSM-5 and HY.

The zeolite Y has a lower conversion but greater selectivity concerning zeolite HBEA, but much less than HZSM-5. This observation may be related to the Brønsted site number (n_1) and strength ($-\Delta H_1$), which are lower than for HBEA, as well as the presence of secondary mesopores in HBEA that facilitate the diffusion. It has been claimed that the density of external sites may collaborate to decrease selectivity in the fructose dehydration under different solvents [19,52]. Cyclic fructose dehydrates quickly on the outer surface of the HY zeolite, which significantly reduces the amount of acyclic fructose that diffuses into the pores. The reaction with external Lewis sites might influence the formation of other products as previously indicated [52]. For example, the regular pore size of the HY zeolite makes it difficult to diffuse out the formed HMF, which favors its rehydration to levulinic and formic acids (consecutive reactions) that can diffuse much more easily within the zeolitic structure [33].

According to literature, density of sites on the external surface of zeolite Y may affect the selectivity of fructose dehydration to form HMF or furfural [52]. Low density of Brønsted sites will favor the furfural formation, whereas high density will favor HMF. Nonetheless, it should be considered that the strength of acid sites on the external surface of HY or HZSM-5 zeolites is much lower than internal surface, as detected by 2,6-di-tert-butylpyridine [46,48], and density is only an average number that not necessarily reflects the actual number of external sites, which is also low compared to the sites in the cavities.

Another relevant issue to the selectivity may be the crystalline domain size. It was observed that it increased with the crystalline domain (D_{XRD}), i.e., larger the size, higher the selectivity (Table 2, D_{XRD}: HZSM-5 > HY > HBEA). A smaller crystallite size favors side reaction, in view of the greater accessibility of the catalytic sites. In microporous materials the external surface acid sites commonly catalyze the reactions in a non-selective manner, which contributes to explaining the observed behavior. Such external surface sites are promptly accessed when there is a smaller crystallite size (higher relative external surface area), which certainly also contributes to the catalytic dehydration in a non-selective way [53].

As we can see, the reactivity of zeolites and amorphous aluminosilicates toward fructose is a complex issue that cannot be rationalized based only in one parameter (e.g., density or strength of acid sites). The adsorption of a molecule such as fructose on the solid is rather on the BAS acid sites due to the higher Gibbs free energy, which is also the strongest sites on the protonic zeolites [46,48]. Accordingly, water molecules inside pores of a zeolitic structure are not homogeneously distributed among Al sites, demonstrated by theoretical and experimental data [54]. Thus, both molecules (fructose and water) will compete for the same adsorption site on the zeolite channels, which will lead to decrease the conversion and selectivity for this dehydration reaction.

3.2. Niobia and HPW Activities

Under typical conditions, fructose dehydration reaction forming HMF develops better using organic solvents to increase conversion and selectivity [55]. However, the amorphous Nb_2O_5 has some fundamental characteristics that favor its use in an aqueous solution. The basic XRD and FT-IR of Py adsorption on the niobia catalysts are presented in Figures S5 and S6. Under the experimental conditions of preparation and treatment, they show only an amorphous halo, while both Brønsted and Lewis sites are present. The Brønsted sites on niobia are located differently than the crystalline aluminosilicates, i.e., mainly on the mesoporous external surface area [56–61]. This characteristic is due to the polarization of the Nb-O bond on the surface polyhedral units, which can facilitate the access of reactants for their transformation into products [56,62]. On the other hand, NbO_4-type sites function as Lewis sites, but this type of site is not available for water [56]. Thus, these Lewis sites are considered water-resistant. The strength of the acidic sites was assessed by microcalorimetry (Table 3, entry 5), which had $-\Delta H_1$ = 88 kJ mol^{-1} and $-\Delta H_2$ = 50 kJ mol^{-1}, with n_1 = 0.06 and n_2 = 0.15 mmol g^{-1} for the Brønsted and Lewis sites, respectively. These data indicate the higher number of Lewis sites accessible on the surface (n_2). Thus, in an aqueous solution, there will be no competition between the solvent and fructose to these Lewis sites, which can be used to improve selectivity. A model of adduct Py-Niobia on the acidic sites has been proposed [25,63], which also agrees with the CO adsorbed on hydrated and dehydrated niobia [22]. Thus, the interaction with Lewis sites is certainly relevant for reactions with different substates.

The textural properties (Table 2) are also an important factor in the dehydration of fructose, as observed for the aluminosilicates. The large distribution of meso- and possible macropores allows the easier diffusion of fructose and products on Brønsted and Lewis sites located on the surface of the pores. The distribution of surface areas are mainly mesopores, as can be observed (Figure 3). Therefore, there are far fewer side reactions than in the case of crystalline aluminosilicates. This assumption suggests that after the formation of the main product (HMF), it is desorbed quickly because of the lower strength of the acidic sites and the larger average pore sizes. This achievement is parallel to the one obtained with mesoporous niobium pentoxide material in the literature [64]. All these properties (adequate strength of sites and high mesoporous surface) probably assist in the obtention of the highest selectivity (28.9%) for pure niobia, among the tested catalysts.

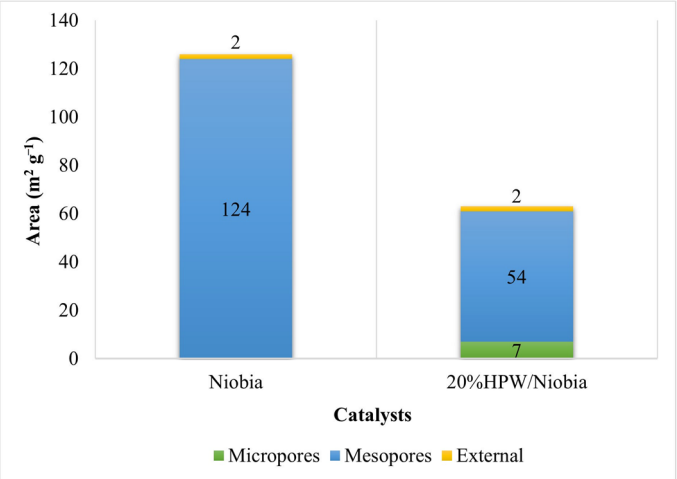

Figure 3. Distribution of specific surface areas of the niobia-based catalysts.

A common modification is to utilize Nb_2O_5 as a support, and in this case we have used it for HPW. Pure HPW in aqueous solution is immediately soluble and deprotonated, so that it behaves like a homogeneous strong acid catalyst like other mineral acids (e.g., HCl, H_2SO_4, H_3PO_4). The conversion results were shown in Table 1 for both pure HPW and

HPW supported on niobia. HPW in a homogeneous solution shows a conversion of 19.3% and selectivity of 34.6%. The high acidity of HPW and probably hydrolysis of the Keggin anion during the reaction time may lead to those results. Even though the selectivity is the highest among the catalysts, the yield is low due to the relatively poor conversion. On the other hand, when we have 20%HPW/Nb_2O_5, the conversion reaches 53.9% and selectivity is 13.4%. The strength and the number of acid sites of 20%HPW/Nb_2O_5 changed significantly, when compared to pure Nb_2O_5, i.e., $-\Delta H_1$ = 85 and $-\Delta H_2$ = 45 kJ mol^{-1}, with n_1 = 0.09 and n_2 = 0.19 mmol g^{-1}. The higher value of n_1 indicates the existence of a greater number of Brønsted sites on the niobia surface, and this agrees with the conversion data that this niobia-based series increased with higher numbers of Brønsted sites (i.e., for n_1: 20%HPW/Nb_2O_5 > Nb_2O_5), whereas the selectivity decreased. This is attributed to the possible deposition of insoluble humins on the catalyst surface, as observed in our carbon balance, as well as indicated in other studies [16]. Brønsted sites can facilitate the conversion of HMF to other by-products, so there was a decrease in selectivity due to side reactions. In addition, the density of the sites (α_{Py} = 2.48 py/nm^2) reveals many more sites distributed on the surface, and this proximity may cause more side reactions than pure niobia, which probably was the cause of a decrease in the selectivity.

At this point, one can observe that there is no simple relationship among acidic strength, number of acid sites, density of acid sites and surface mesoporous areas among these different catalysts. Nonetheless, we have stablished that a right combination of these parameters in one catalyst may lead to a better conversion and mainly selectivity to HMF. Thus, the optimum acidity strength ($-\Delta H_1$) of catalysts should be between 80 to 100 kJ mol^{-1}, with about 0.20 to 0.30 mmol g^{-1} of acid sites, density about 1 site nm^{-2} and mesoporous area about 100 m^2 g^{-1}. These values fit well within the general order of the selectivity (i.e., Nb_2O_5 > HZSM-5 > 20%HPW/Nb_2O_5 > SiO_2-Al_2O_3 > HY > HBEA).

Besides this, niobia was also shown to be the most efficient catalyst based on the turnover numbers (Table 4). Thus, on all measured criteria (TON, conversion, selectivity and yield) this catalyst showed the best performance among the tested ones.

$$\mathrm{TON(Fructose)} = \frac{n_{\text{initial fructose}}\,(\mathrm{mol}) \times \mathrm{conversion}/100}{n_{\text{acid sites}}\,(\mathrm{mol/g}) \times \text{catalyst mass(g)}}$$

$$\mathrm{TON(Fructose)} = \frac{n_{\text{initial fructose}}\,(\mathrm{mol}) \times \mathrm{yield}/100}{n_{\text{acid sites}}\,(\mathrm{mol/g}) \times \text{catalyst mass(g)}}$$

Table 4. Turnover number [a] for fructose reaction and HMF formation for the different catalysts in aqueous solution reaction (120 °C, 2 h; 1.0 g fructose; 0.1 g catalyst; 30 mL deionized water).

Catalyst	TON (Fructose)	TON (HMF)
HBEA	18,013	1152
HY	20,184	1850
SiO_2-Al_2O_3	10,056	1110
HZSM-5	13,111	2297
Nb_2O_5 (amorphous)	125,550	36,211
20%HPW/Nb_2O_5	110,869	14,884
HPW	10,301	3576

[a] Ratio between the number of moles of fructose consumed or HMF produced and the total number of catalytic acid sites (n_T, calorimetric analysis).

A preliminary recycle study of the niobia catalyst was performed for three reutilizations. The results show conversion of 47.5%, 42.4% and 30.1% in cycles one to three, respectively, whereas the selectivity was 28.9%, 35.2% and 23.6% for the sequential reutilization. The treatment between the cycles were not much elaborated, i.e., it only consisted of thoroughly washing the catalyst with deionized water and heating at 100 °C for 4 h before reinserted it in the reactor. The level of deactivation is within the observed level in

another report for niobia-based catalysts for the same reaction [65], which indicates a fair stability for this catalyst.

3.3. Comparison with Other Catalysts for Aqueous Fructose Dehydration

A brief comparison among the various catalysts tested using batch conditions in the same dehydration reaction is presented in Table 5. First, one should be aware that the conditions are not exactly the same in all the taken examples. Then, it can be noted that the system tested here with niobia treated at 100 °C for one hour has one of the highest yields (13.7%) in a relatively short reaction time (two hours). Niobia-based catalysts [16,66,67] and supported WO_3 on zirconia [16,68] also demonstrated promising results. In a recent study, solid acid TiO_2-SO_3H showed a very high selectivity (71%) using low fructose concentration (0.1 mol L^{-1}), 18 mg of catalyst at 140 °C for 1 h [26]. This result also reveals the potential for further development of this type of catalyst. It should be noted, moreover, that the apparently most efficient catalysts (e.g., HCl, H_2SO_4) are not environmentally friendly and not recyclable because of the homogeneous conditions of the reaction.

Table 5. A simplified comparison among various catalysts in fructose dehydration to HMF under aqueous solution.

Catalyst	HMF Yield (%)	Temperature (°C)	Time (h)	Ratio [a] (%)	Reference
Nb_2O_5	13.7	120	2	10	This work
Nb_2O_5	7.3	120	2	10	[66]
$NbO(OH)_3$	10.0	150	2	5	[16]
NbPW (0.6 Nb/P)	7.8	80	3	33	[67]
$Cs_2HPW_{12}O_{40}$	4.0	150	2	5	[16]
ZrO_2	8.0	130	4	13.3	[68]
16.8% WO_3/ZrO_2	12.0	130	4	13.3	[68]
12% WO_3/ZrO_2	7.0	150	2	5	[16]
ZSM-5 (hierarchical)	9.8	130	4	13.3	[69]
BEA (hierarchical)	3.2	130	4	13.3	[69]
USY (hierarchical)	8.3	130	4	13.3	[69]
Porous Carbon-SO_3H	2.5	110	4	10	[70]
TiO_2-SO_3H	4.0	140	1	11.1	[26]
HCl or H_2SO_4 [b]	40	120	-	b	[55]

[a] Ratio Catalyst/Fructose (wt.%). [b] HMF yield values at ~90% conversion. Molar ratio of Catalyst/Fructose = 10.

4. Conclusions

Several catalysts were tested in the reaction of fructose dehydration for HMF, providing a complete examination of its behavior in an aqueous medium, which grants a green and sustainable protocol for such transformation. All classes of catalysts proved to be efficient and better than the non-catalytic process. Moreover, it became clear how the strength and accessibility of acidic sites, as well as the nature of the sites (Brønsted and Lewis), were essential for the results. A synergistic effect of the acidity (strength, number and density of the sites) and shape selectivity (especially when comparing the aluminosilicates) are key factors in designing solid acids consistent with high conversion and yield for HMF. However, reactivity of all tested catalysts toward fructose is complex and cannot be rationalized based only on one parameter (e.g., strength, number, density of acid sites) and textural parameters are also important to improve its selectivity. Among the zeolites, the yield was approximately proportional to the acid strength. However, other catalysts, even with weaker sites, obtained better results due to the textural characteristics (mesoporous area distribution), accessibility and stability of the sites (e.g., amorphous silica-alumina, niobic acid). Niobic acid ($Nb_2O_5 \cdot nH_2O$) was the best among the tested catalysts (highest TON, yield, selectivity and conversion). The use of HPW as a catalyst has thrown up good results, but it is known that the use of homogeneous catalysis creates several drawbacks, such as difficulty in separating and reusing the catalyst. The association between HPW and niobic acid brought about high activity, but the TON for HMF declined, which was associated with consecutive reactions favored by a higher density of Brønsted

acid sites. Optimum strength, accessibility and stability of the acid sites should be sought to achieve the most efficient catalyst for fructose transformation into HMF.

Supplementary Materials: The supplementary data are available online at https://www.mdpi.com/article/10.3390/chemistry3040087/s1. Figure S1: Analytical curves of fructose (a) and HMF (b), Figure S2: XRD patterns of the aluminosilicates, Figure S3: FT-IR spectra of (A) crystalline aluminosilicates and (B) amorphous silica-alumina after adsorption of pyridine, Figure S4: Adsorption and desorption isotherms of N_2 at −196 °C of the catalysts.

Author Contributions: J.P.V.L. performed and participated in most of the conceptualization of the experimental work as part of his Master's Thesis. P.T.A.C. helped in the reaction experiments and preparation of catalysts. M.F.P. aided in the XRD, FT-IR and textural analyses. J.J.L. contributed to the development of HPLC methods of analysis. S.C.L.D. participated in the conceptualization and funding acquisition. J.A.D. coordinated the work and wrote the first drafts of the paper; he was also responsible for funding acquisition. All authors assisted equally in article revision, data interpretation and discussion of the results. All authors have read and agreed to the published version of the manuscript.

Funding: CNPq (grants no. 307845/2019-2 and 307091/2018-0) and CAPES (grant no. 001) for research and graduate student scholarships, and the financial support provided by DPI/IQ/UnB, MCTIC/CNPq (grant no. 480165/2013-0 and 484384/2012-0), CAPES, FAPDF (grant no. 0193.001799/2017 and 0193.001348/2016), FINATEC, FINEP/CTPetro/CTInfra and Petrobras.

Institutional Review Board Statement: Not applicable.

Informed Consent Statement: Not applicable.

Data Availability Statement: Data from experiments can be accessed from Supplementary Information.

Acknowledgments: We would like to thank Richieli Vieira (commercial development coordinator, PQ Silicas Brazil) for providing zeolites.

Conflicts of Interest: The authors declare no competing financial or any other conflict of interest.

References

1. Sørensen, B. A history of renewable energy technology. *Energy Policy* **1991**, *19*, 8–12. [CrossRef]
2. Bulut, U. The impacts of non-renewable and renewable energy on CO_2 emissions in Turkey. *Environ. Sci. Pollut. Res.* **2017**, *24*, 15416–15426. [CrossRef]
3. Christensen, C.H.; Rass-Hansen, J.; Marsden, C.C.; Taarning, E.; Egeblad, K. The Renewable Chemicals Industry. *ChemSusChem* **2008**, *1*, 283–289. [CrossRef]
4. Kharaka, Y.K.; Dorsey, N.S. Environmental issues of petroleum exploration and production: Introduction. *Environ. Geosci.* **2005**, *12*, 61–63. [CrossRef]
5. Koçak, E.; Şarkgüneşi, A. The impact of foreign direct investment on CO_2 emissions in Turkey: New evidence from cointegration and bootstrap causality analysis. *Environ. Sci. Pollut. Res.* **2018**, *25*, 790–804. [CrossRef]
6. Klass, D. Biomass as an Energy Resource: Concept and Markets. In *Biomass for Renewable Energy, Fuels, and Chemicals*; Elsevier: San Diego, CA, USA, 1998; pp. 29–50.
7. Ližbetin, J.; Hlatká, M.; Bartuška, L. Issues Concerning Declared Energy Consumption and Greenhouse Gas Emissions of FAME Biofuels. *Sustainability* **2018**, *10*, 3025. [CrossRef]
8. Ge, J.; Yoon, S.; Choi, N. Using Canola Oil Biodiesel as an Alternative Fuel in Diesel Engines: A Review. *Appl. Sci.* **2017**, *7*, 881. [CrossRef]
9. van Putten, R.-J.; van der Waal, J.C.; de Jong, E.; Rasrendra, C.B.; Heeres, H.J.; de Vries, J.G. Hydroxymethylfurfural, A Versatile Platform Chemical Made from Renewable Resources. *Chem. Rev.* **2013**, *113*, 1499–1597. [CrossRef] [PubMed]
10. Lucas, N.; Kokate, G.; Nagpure, A.; Chilukuri, S. Dehydration of fructose to 5-hydroxymethyl furfural over ordered AlSBA-15 catalysts. *Microporous Mesoporous Mater.* **2013**, *181*, 38–46. [CrossRef]
11. Wang, T.; Nolte, M.W.; Shanks, B.H. Catalytic dehydration of C 6 carbohydrates for the production of hydroxymethylfurfural (HMF) as a versatile platform chemical. *Green Chem.* **2014**, *16*, 548–572. [CrossRef]
12. Lv, G.; Deng, L.; Lu, B.; Li, J.; Hou, X.; Yang, Y. Efficient dehydration of fructose into 5-hydroxymethylfurfural in aqueous medium over silica-included heteropolyacids. *J. Clean. Prod.* **2017**, *142*, 2244–2251. [CrossRef]
13. Kruger, J.S.; Choudhary, V.; Nikolakis, V.; Vlachos, D.G. Elucidating the Roles of Zeolite H-BEA in Aqueous-Phase Fructose Dehydration and HMF Rehydration. *ACS Catal.* **2013**, *3*, 1279–1291. [CrossRef]

14. Qi, X.; Watanabe, M.; Aida, T.M.; Smith, R.L. Sulfated zirconia as a solid acid catalyst for the dehydration of fructose to 5-hydroxymethylfurfural. *Catal. Commun.* **2009**, *10*, 1771–1775. [CrossRef]
15. Haque, M.A.; Yang, X.; Ong, K.L.; Tang, W.-T.; Kwan, T.H.; Kulkarni, S.; Lin, C.S.K. Bioconversion of beverage waste to high fructose syrup as a value-added product. *Food Bioprod. Process.* **2017**, *105*, 179–187. [CrossRef]
16. de Souza, R.L.; Yu, H.; Rataboul, F.; Essayem, N. 5-Hydroxymethylfurfural (5-HMF) Production from Hexoses: Limits of Heterogeneous Catalysis in Hydrothermal Conditions and Potential of Concentrated Aqueous Organic Acids as Reactive Solvent System. *Challenges* **2012**, *3*, 212–232. [CrossRef]
17. Choudhary, V.; Burnett, R.I.; Vlachos, D.G.; Sandler, S.I. Dehydration of Glucose to 5-(Hydroxymethyl)furfural and Anhydroglucose: Thermodynamic Insights. *J. Phys. Chem. C* **2012**, *116*, 5116–5120. [CrossRef]
18. Guo, J.; Zhu, S.; Cen, Y.; Qin, Z.; Wang, J.; Fan, W. Ordered mesoporous Nb–W oxides for the conversion of glucose to fructose, mannose and 5-hydroxymethylfurfural. *Appl. Catal. B Environ.* **2017**, *200*, 611–619. [CrossRef]
19. Ordomsky, V.V.; van der Schaaf, J.; Schouten, J.C.; Nijhuis, T.A. The effect of solvent addition on fructose dehydration to 5-hydroxymethylfurfural in biphasic system over zeolites. *J. Catal.* **2012**, *287*, 68–75. [CrossRef]
20. Thananatthanachon, T.; Rauchfuss, T.B. Efficient Production of the Liquid Fuel 2,5-Dimethylfuran from Fructose Using Formic Acid as a Reagent. *Angew. Chem.* **2010**, *122*, 6766–6768. [CrossRef]
21. Prat, D.; Wells, A.; Hayler, J.; Sneddon, H.; McElroy, C.R.; Abou-Shehada, S.; Dunn, P.J. CHEM21 selection guide of classical- and less classical-solvents. *Green Chem.* **2016**, *18*, 288–296. [CrossRef]
22. Nakajima, K.; Baba, Y.; Noma, R.; Kitano, M.; Kondo, J.N.; Hayashi, S.; Hara, M. $Nb_2O_5{\cdot}nH_2O$ as a Heterogeneous Catalyst with Water-Tolerant Lewis Acid Sites. *J. Am. Chem. Soc.* **2011**, *133*, 4224–4227. [CrossRef]
23. Karinen, R.; Vilonen, K.; Niemelä, M. Biorefining: Heterogeneously Catalyzed Reactions of Carbohydrates for the Production of Furfural and Hydroxymethylfurfural. *ChemSusChem* **2011**, *4*, 1002–1016. [CrossRef]
24. Zhong, J.; Pérez-Ramírez, J.; Yan, N. Biomass valorisation over polyoxometalate-based catalysts. *Green Chem.* **2021**, *23*, 18–36. [CrossRef]
25. Kreissl, H.T.; Nakagawa, K.; Peng, Y.-K.; Koito, Y.; Zheng, J.; Tsang, S.C.E. Niobium oxides: Correlation of acidity with structure and catalytic performance in sucrose conversion to 5-hydroxymethylfurfural. *J. Catal.* **2016**, *338*, 329–339. [CrossRef]
26. Testa, M.L.; Miroddi, G.; Russo, M.; la Parola, V.; Marcì, G. Dehydration of Fructose to 5-HMF over Acidic TiO2 Catalysts. *Materials* **2020**, *13*, 1178. [CrossRef] [PubMed]
27. Valadares, D.S.; Clemente, M.C.H.; de Freitas, E.F.; Martins, G.A.V.; Dias, J.A.; Dias, S.C.L. Niobium on BEA Dealuminated Zeolite for High Selectivity Dehydration Reactions of Ethanol and Xylose into Diethyl Ether and Furfural. *Nanomaterials* **2020**, *10*, 1269. [CrossRef]
28. Okuhara, T. Water-Tolerant Solid Acid Catalysts. *Chem. Rev.* **2002**, *102*, 3641–3666. [CrossRef]
29. Assary, R.S.; Redfern, P.C.; Hammond, J.R.; Greeley, J.; Curtiss, L.A. Computational Studies of the Thermochemistry for Conversion of Glucose to Levulinic Acid. *J. Phys. Chem. B* **2010**, *114*, 9002–9009. [CrossRef] [PubMed]
30. Vieira, J.L.; Almeida-Trapp, M.; Mithöfer, A.; Plass, W.; Gallo, J.M.R. Rationalizing the conversion of glucose and xylose catalyzed by a combination of Lewis and Brønsted acids. *Catal. Today* **2020**, *344*, 92–101. [CrossRef]
31. Patil, S.K.R.; Lund, C.R.F. Formation and Growth of Humins via Aldol Addition and Condensation during Acid-Catalyzed Conversion of 5-Hydroxymethylfurfural. *Energy Fuels* **2011**, *25*, 4745–4755. [CrossRef]
32. Dutta, S.; De, S.; Saha, B. Advances in biomass transformation to 5-hydroxymethylfurfural and mechanistic aspects. *Biomass Bioenergy* **2013**, *55*, 355–369. [CrossRef]
33. Ordomsky, V.V.; van der Schaaf, J.; Schouten, J.C.; Nijhuis, T.A. Fructose Dehydration to 5-Hydroxymethylfurfural over Solid Acid Catalysts in a Biphasic System. *ChemSusChem* **2012**, *5*, 1812–1819. [CrossRef]
34. Nogueira, J.S.M.; Santana, V.T.; Henrique, P.V.; de Aguiar, L.G.; Silva, J.P.A.; Mussatto, S.I.; Carneiro, L.M. Production of 5-Hydroxymethylfurfural from Direct Conversion of Cellulose Using Heteropolyacid/Nb2O5 as Catalyst. *Catalysts* **2020**, *10*, 1417. [CrossRef]
35. Chang, C.-C.; Je Cho, H.; Yu, J.; Gorte, R.J.; Gulbinski, J.; Dauenhauer, P.; Fan, W. Lewis acid zeolites for tandem Diels–Alder cycloaddition and dehydration of biomass-derived dimethylfuran and ethylene to renewable p-xylene. *Green Chem.* **2016**, *18*, 1368–1376. [CrossRef]
36. Primo, A.; Garcia, H. Zeolites as catalysts in oil refining. *Chem. Soc. Rev.* **2014**, *43*, 7548–7561. [CrossRef] [PubMed]
37. Corma, A. From Microporous to Mesoporous Molecular Sieve Materials and Their Use in Catalysis. *Chem. Rev.* **1997**, *97*, 2373–2420. [CrossRef] [PubMed]
38. Corma, A. Inorganic Solid Acids and Their Use in Acid-Catalyzed Hydrocarbon Reactions. *Chem. Rev.* **1995**, *95*, 559–614. [CrossRef]
39. Guisnet, M.R. Model reactions for characterizing the acidity of solid catalysts. *Acc. Chem. Res.* **1990**, *23*, 392–398. [CrossRef]
40. Zhuravlev, L.T. The surface chemistry of amorphous silica. Zhuravlev model. *Colloids Surf. A Physicochem. Eng. Asp.* **2000**, *173*, 1–38. [CrossRef]
41. Yi, F.; Chen, Y.; Tao, Z.; Hu, C.; Yi, X.; Zheng, A.; Wen, X.; Yun, Y.; Yang, Y.; Li, Y. Origin of weak Lewis acids on silanol nests in dealuminated zeolite Beta. *J. Catal.* **2019**, *380*, 204–214. [CrossRef]

42. Caratzoulas, S.; Davis, M.E.; Gorte, R.J.; Gounder, R.; Lobo, R.F.; Nikolakis, V.; Sandler, S.I.; Snyder, M.A.; Tsapatsis, M.; Vlachos, D.G. Challenges of and Insights into Acid-Catalyzed Transformations of Sugars. *J. Phys. Chem. C* **2014**, *118*, 22815–22833. [CrossRef]
43. Zhang, J.; Weitz, E. An in Situ NMR Study of the Mechanism for the Catalytic Conversion of Fructose to 5-Hydroxymethylfurfural and then to Levulinic Acid Using 13C Labeled d -Fructose. *ACS Catal.* **2012**, *2*, 1211–1218. [CrossRef]
44. Wang, M.; Xia, Y.; Zhao, L.; Song, C.; Peng, L.; Guo, X.; Xue, N.; Ding, W. Remarkable acceleration of the fructose dehydration over the adjacent Brønsted acid sites contained in an MFI-type zeolite channel. *J. Catal.* **2014**, *319*, 150–154. [CrossRef]
45. Janda, A.; Bell, A.T. Effects of Si/Al Ratio on the Distribution of Framework Al and on the Rates of Alkane Monomolecular Cracking and Dehydrogenation in H-MFI. *J. Am. Chem. Soc.* **2013**, *135*, 19193–19207. [CrossRef] [PubMed]
46. Drago, R.S.; Dias, S.C.; Torrealba, M.; de Lima, L. Calorimetric and Spectroscopic Investigation of the Acidity of HZSM-5. *J. Am. Chem. Soc.* **1997**, *119*, 4444–4452. [CrossRef]
47. Freitas, E.F.; Araújo, Á.A.L.; Paiva, M.F.; Dias, S.C.L.; Dias, J.A. Comparative acidity of BEA and Y zeolite composites with 12-tungstophosphoric and 12-tungstosilicic acids. *Mol. Catal.* **2018**, *458*, 152–160. [CrossRef]
48. Loureiro Dias, S.C.; de Macedo, J.L.; Dias, J.A. Acidity measurements of zeolite Y by adsorption of several probes. *Phys. Chem. Chem. Phys.* **2003**, *5*, 5574–5579. [CrossRef]
49. De Mattos, F.C.G.; de Carvalho, E.N.C.B.; de Freitas, E.F.; Paiva, M.F.; Ghesti, G.F.; de Macedo, J.L.; Dias, S.C.L.; Dias, J.A. Acidity and Characterization of 12-Tungstophosphoric Acid Supported on Silica-Alumina. *J. Braz. Chem. Soc.* **2016**, *28*, 336–347. [CrossRef]
50. Caliman, E.; Dias, J.A.; Dias, S.C.L.; Garcia, F.A.C.; de Macedo, J.L.; Almeida, L.S. Preparation and characterization of $H_3PW_{12}O_{40}$ supported on niobia. *Microporous Mesoporous Mater.* **2010**, *132*, 103–111. [CrossRef]
51. Weingarten, R.; Cho, J.; Xing, R.; Conner, W.C.; Huber, G.W. Kinetics and Reaction Engineering of Levulinic Acid Production from Aqueous Glucose Solutions. *ChemSusChem* **2012**, *5*, 1280–1290. [CrossRef]
52. Wang, L.; Guo, H.; Xie, Q.; Wang, J.; Hou, B.; Jia, L.; Cui, J.; Li, D. Conversion of fructose into furfural or 5-hydroxymethylfurfural over HY zeolites selectively in γ-butyrolactone. *Appl. Catal. A Gen.* **2019**, *572*, 51–60. [CrossRef]
53. Singh, M.; Kamble, R.; Viswanadham, N. Effect of Crystal Size on Physico-Chemical Properties of ZSM-5. *Catal. Lett.* **2008**, *120*, 288–293. [CrossRef]
54. Stanciakova, K.; Weckhuysen, B.M. Water–active site interactions in zeolites and their relevance in catalysis. *Trends Chem.* **2021**, *3*, 456–468. [CrossRef]
55. Mellmer, M.A.; Sanpitakseree, C.; Demir, B.; Ma, K.; Elliott, W.A.; Bai, P.; Johnson, R.L.; Walker, T.W.; Shanks, B.H.; Rioux, R.M.; et al. Effects of chloride ions in acid-catalyzed biomass dehydration reactions in polar aprotic solvents. *Nat. Commun.* **2019**, *10*, 1132. [CrossRef] [PubMed]
56. Nowak, I.; Ziolek, M. Niobium Compounds: Preparation, Characterization, and Application in Heterogeneous Catalysis. *Chem. Rev.* **1999**, *99*, 3603–3624. [CrossRef] [PubMed]
57. Maurer, S. Structural and acidic characterization of niobia aerogels. *J. Catal.* **1992**, *135*, 125–134. [CrossRef]
58. Wachs, I.E.; Jehng, J.-M.; Deo, G.; Hu, H.; Arora, N. Redox properties of niobium oxide catalysts. *Catal. Today* **1996**, *28*, 199–205. [CrossRef]
59. Jehng, J.M.; Wachs, I.E. Molecular structures of supported niobium oxide catalysts under in situ conditions. *J. Phys. Chem.* **1991**, *95*, 7373–7379. [CrossRef]
60. Batamack, P.; Vincent, R.; Fraissard, J. Niobium oxide acidity studied by proton broad-line NMR at 4 K and MAS NMR at room temperature. *Catal. Lett.* **1996**, *36*, 81–86. [CrossRef]
61. Tanabe, K. Niobic acid as an unusual acidic solid material. *Mater. Chem. Phys.* **1987**, *17*, 217–225. [CrossRef]
62. Tanabe, K. Catalytic application of niobium compounds. *Catal. Today* **2003**, *78*, 65–77. [CrossRef]
63. Martins, J.B.L.; Fialho, T.A.S. Interaction of pyridine on Nb2O5. *J. Mol. Struct.* **2005**, *732*, 1–5. [CrossRef]
64. García-Sancho, C.; Rubio-Caballero, J.M.; Mérida-Robles, J.M.; Moreno-Tost, R.; Santamaría-González, J.; Maireles-Torres, P. Mesoporous Nb_2O_5 as solid acid catalyst for dehydration of d-xylose into furfural. *Catal. Today* **2014**, *234*, 119–124. [CrossRef]
65. do Prado, N.T.; Souza, T.E.; Machado, A.R.T.; Souza, P.P.; Monteiro, R.S.; Oliveira, L.C.A. Enhanced catalytic activity for fructose conversion on nanostructured niobium oxide after hydrothermal treatment: Effect of morphology and porous structure. *J. Mol. Catal. A Chem.* **2016**, *422*, 23–34. [CrossRef]
66. Wang, F.; Wu, H.-Z.; Liu, C.-L.; Yang, R.-Z.; Dong, W.-S. Catalytic dehydration of fructose to 5-hydroxymethylfurfural over Nb_2O_5 catalyst in organic solvent. *Carbohydr. Res.* **2013**, *368*, 78–83. [CrossRef]
67. Qiu, G.; Wang, X.; Huang, C.; Li, Y.; Chen, B. Niobium phosphotungstates: Excellent solid acid catalysts for the dehydration of fructose to 5-hydroxymethylfurfural under mild conditions. *RSC Adv.* **2018**, *8*, 32423–32433. [CrossRef]
68. Kourieh, R.; Rakic, V.; Bennici, S.; Auroux, A. Relation between surface acidity and reactivity in fructose conversion into 5-HMF using tungstated zirconia catalysts. *Catal. Commun.* **2013**, *30*, 5–13. [CrossRef]
69. Rac, V.; Rakić, V.; Stošić, D.; Otman, O.; Auroux, A. Hierarchical ZSM-5, Beta and USY zeolites: Acidity assessment by gas and aqueous phase calorimetry and catalytic activity in fructose dehydration reaction. *Microporous Mesoporous Mater.* **2014**, *194*, 126–134. [CrossRef]
70. Wang, L.; Zhang, J.; Zhu, L.; Meng, X.; Xiao, F.-S. Efficient conversion of fructose to 5-hydroxymethylfurfural over sulfated porous carbon catalyst. *J. Energy Chem.* **2013**, *22*, 241–244. [CrossRef]